

## Dataset collection from a SubT environment<sup>☆</sup>

Anton Koval<sup>a,\*</sup>, Samuel Karlsson<sup>a</sup>, Sina Sharif Mansouri<sup>a</sup>, Christoforos Kanellakis<sup>a</sup>, Ilias Tevetzidis<sup>a</sup>, Jakub Haluska<sup>a</sup>, Ali-akbar Agha-mohammadi<sup>b</sup>, George Nikolakopoulos<sup>a</sup>

<sup>a</sup> Robotics & AI Team, Department of Computer, Electrical and Space Engineering, Luleå, University of Technology, Luleå SE-97187, Sweden

<sup>b</sup> Jet Propulsion Laboratory California Institute of Technology Pasadena, CA, 91109, United States of America

### ARTICLE INFO

#### Article history:

Received 28 September 2021

Received in revised form 31 March 2022

Accepted 28 May 2022

Available online 14 June 2022

#### Keywords:

Dataset

SubT

RGB

RGB-D

Event-based and thermal cameras

2D and 3D lidars

### ABSTRACT

This article presents a dataset collected from the subterranean (SubT) environment with a current state-of-the-art sensors required for autonomous navigation. The dataset includes sensor measurements collected with RGB, RGB-D, event-based and thermal cameras, 2D and 3D lidars, inertial measurement unit (IMU), and ultra wideband (UWB) positioning systems which are mounted on the mobile robot. The overall sensor setup will be referred further in the article as a data collection platform. The dataset contains synchronized raw data measurements from all the sensors in the robot operating system (ROS) message format and video feeds collected with action and 360 cameras. A detailed description of the sensors embedded into the data collection platform and a data collection process are introduced. The collected dataset is aimed for evaluating navigation, localization and mapping algorithms in SubT environments. This article is accompanied with the public release of all collected datasets from the SubT environment. Link: [Dataset](#)

© 2022 The Author(s). Published by Elsevier B.V. This is an open access article under the CC BY license (<http://creativecommons.org/licenses/by/4.0/>).

## 1. Introduction

Robots, operating in subterranean (SubT) environments, should be able to cope with harsh environmental conditions to successfully complete their mission [1,2]. Usually, this type of an environment has poor illumination conditions, unconditioned narrow passages and crossing paths, dirt, high humidity, and dust [3]. Fig. 1 illustrates an example of an underground tunnel in Sweden to indicate the low illumination levels, as well as the uneven wall surfaces. In order to achieve successful mission with robots, there is a need to evaluate different sensor suites in SubT environments.

Subterranean environment navigation gained a lot of attention with the announcement of the SubT Challenge [4,5]. The main goal of this competition is to foster technological breakthroughs in mapping, navigation and exploration approaches for enabling autonomous robot operations in harsh subterranean environments like human-made tunnels, urban undergrounds, and natural caves. The competing teams in the DARPA SubT Challenge [1,6–11] were tackling robotic challenges in the underground domain, with an outstanding push of their autonomy levels. Teams in the final competition deployed autonomous ground

and aerial robotic platforms designated to identify and localize artefacts on the explored map. For that, they developed both hardware and software solutions addressing capabilities related to multi-modal perception, path planning, reactive navigation, determining terrain traversability under degrading sensing in dark areas, self-similar environments, and extreme terrains. To tackle these challenges and motivate the development of new robotic capabilities there is a constant need for versatile datasets from SubT environments with various system modalities that include both state-of-the-art and novel sensors.

Until now and to the best of the authors knowledge, there are two datasets from mining environments that contain measurements from multiple sensors. One is from Chilean underground mine [12]. However, its sensor set is limited to stereo camera, 3D lidar and 2D radar. Another published dataset is from Kvarntorp mine [13], in which sensor configuration is limited to a 3D lidar. Moreover, recently, the teams that participated in the DARPA SubT Challenge have publicly released datasets for the evaluation of perception and SLAM algorithms in harsh SubT environments, such as the OIVIO dataset [14] which provides stereo camera and vertical reference sensor data, the Tunnel-Circuit dataset [15] providing data from 3D lidar, IMU and omnidirectional camera, the Robotic Interestingness dataset [16] which includes data from 3D lidar and camera, as well as the SubT Reference Dataset [17,18] provides data from the tunnel and urban circuits while more specifically including 3D lidars, IMU, thermal and stereo camera sensors. In [19] there is also a collection of data resources from underground environments including tunnel circuit. However, none of the upper-mentioned datasets is including data

<sup>☆</sup> This work has been partially funded by the European Unions Horizon 2020 Research and Innovation Programme under the Grant Agreement No. 869379 illuMINEation.

\* Corresponding author.

E-mail address: [antkov@ltu.se](mailto:antkov@ltu.se) (A. Koval).



**Fig. 1.** Sample data output from the Luleå underground tunnel, collected with the Intel RealSense D455 camera — first row. In the second row are shown data outputs from an Intel RealSense T265, a thermal camera FLIR Boson 640, a Prophesse event camera and a 3D lidar Velodyne Puck Lite.

from event trigger camera. So, there is a need of introducing a dataset with multiple visual and ranging sensors, as well as with event trigger camera that can be used for the development and evaluation of navigation and mapping algorithms that will enable autonomous robots' operations in SubT environments. Worth noting that all SubT-based datasets except OIVIO [14] are released in ROS bag format,<sup>1</sup> while, the authors of the OIVIO dataset provide scripts to convert the data into the ROS bag format. Thus, in this study, the introduced dataset has ROS bag format, which makes it consistent with the released datasets from the DARPA SubT Challenge.

This article presents the dataset collected from Luleå Sweden underground tunnel with 9 sensors compatible with the robot operating system (ROS), including inertial measurement unit (IMU), ultra wideband (UWB), 2D and 3D lidars, thermal, stereo, depth, and event cameras, which were assembled in the data collection platform and mounted on the Pioneer 3-AT robot as depicted on Fig. 2(b). The main aim and merit of this work is to provide and support the robotics community with a variety of sensor data in limited to public SubT areas, towards the deployment of robotic systems in challenging underground environments. The sensor suite for the dataset collection is designed to capture a big spectrum of data types, including both conventional sensors like RGB and depth cameras, as well as novel sensors, like event cameras, for the first time ever, to allow further developments and bench-marking of related algorithms. All sensor measurements are stored and serialized in a standard ROS bag file format. Structurally, the dataset is divided into 3 parts for 3 sensors' sets during which the data were recorded with manually controlled robot. Each dataset part contains bag files storing measurements from individual sensors set. Additionally, the dataset includes video feed data from action and 360 cameras.

The rest of the article is structured as follows. Section 2 describes the sensors used for data collection and robotic platform, while Section 3 introduces the SubT area description. Finally, Section 4 provides details about the data format, collection process and usage.

## 2. Data collection platform

This Section will introduce the mobile robot and sensors embedded in the data collection platform.

The Pioneer 3-AT<sup>2</sup> was used for collecting the dataset. It is a four wheel drive robot capable of carrying nearly 30 kg of payload

and climb a 60% grade. The data collection platform incorporates sensor tower consisting of a 3D lidar, 2D lidar, UWB node, RGB, RGB-D, event, thermal, action and 360 cameras, all placed in the front part of its upper deck. The onboard Intel NUC computer with batteries for powering the data collection platform were respectively placed in the middle and in the back of the upper deck. To provide an unobstructed view on the environment all sensors were mounted as a column structure and visual sensors were mounted in a front looking position with separate LED light bars Lustrean DV12V 10 W with dimensions 170 × 15 mm pointing towards the field of view of each camera. The sensor placement on the Pioneer 3-AT is depicted in Fig. 2(a), while all sensors specifications are summarized in Table 2. Prior to the dataset collection, all the sensors were staying for 20 min in the tunnel environment. This time is required for the internal thermal camera's processing engine to perform re-calibration in order to produce optimal image quality.

### 2.1. Vision sensors

This subsection introduces sensors that can be equipped on ground robots and unmanned aerial vehicles, with typical application areas to include collision avoidance, 3D scanning, volumetric measurements, position estimation, simultaneous localization and mapping (SLAM), thermal imaging etc.

For collecting RGB images and evaluating the visual odometry methods, the Intel RealSense T265<sup>3</sup> has been selected. This is a lightweight sensor with low power consumption that includes two fisheye lens sensors with resolution 848 × 800 pixels, an IMU with sample rate of 0.005 sec and a vision processing unit (VPU).

The RealSense D455<sup>4</sup> depth camera has an IMU with a sample rate of 0.005 sec, a RGB camera with 1280 × 800 at 30 fps and a depth camera with an IR projector to collect the depth data up to 1280 × 720 pixels.

Prophesse EVALUATION KIT — Gen3M VGA-CD 1.1 is an event trigger camera that provides up to 5 KHz asynchronous pixel wise events, a high dynamic range, and enables to capture events with low illumination of 0.08 lx and has a resolution of 640 × 480 pixels. The camera intrinsic calibrations were performed with the Prophesses calibration tool,<sup>5</sup> while in Table 1 the event camera utilized biases were shown.

The FLIR Boson 640 longwave infrared (LWIR) professional grade thermographic camera senses infrared radiation, which makes it suitable for low light environments. It is equipped with

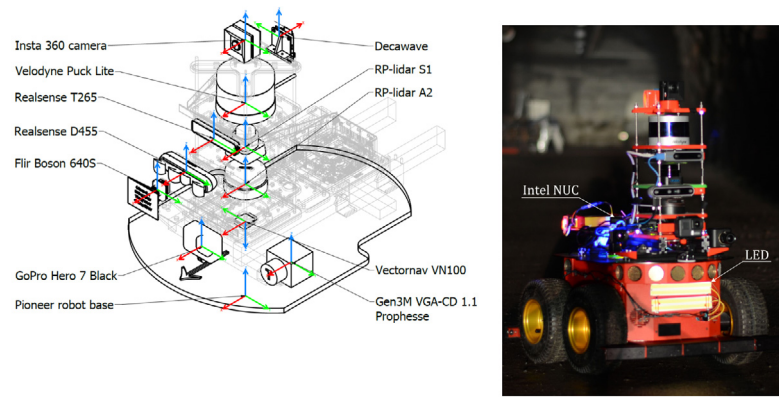
<sup>1</sup> <http://wiki.ros.org/rosbag>

<sup>2</sup> <https://www.generationrobots.com/media/Pioneer3AT-P3AT-RevA-datasheet.pdf>

<sup>3</sup> <https://www.intelrealsense.com/tracking-camera-t265/>

<sup>4</sup> <https://www.intelrealsense.com/depth-camera-d455/>

<sup>5</sup> [https://docs.prophesse.ai/stable/metavision\\_sdk/](https://docs.prophesse.ai/stable/metavision_sdk/)



(a) Sensors' static reference frames.  $x$ ,  $y$  and  $z$  axes are represented with red, green and blue colours respectively

(b) Pioneer 3 AT equipped with sensors for dataset collection in the underground tunnel.

Fig. 2. Data collection platform.

Table 1

Event camera bias used during data collection.

bias_refr	1800
bias_hpf	2600
bias_diff_off	220
bias_diff_on	460
bias_diff	300
bias_fo	1670
bias_pr	1500

4.9 mm lens and has a resolution of  $640 \times 512$  pixels, a frame rate of 60 Hz and a thermal sensitivity of  $< 50$  mK.

Furthermore, the action camera GoPro Hero7 Black camera is used, which provides videos of  $3840 \times 2160$  pixels with 60 fps.

The Insta 360 EVO camera is capable to provide omnidirectional videos with resolution up to  $5760 \times 2880$  at 30 fps and images with a resolution of  $6080 \times 3040$ .

## 2.2. Infrared ranging sensors

This subsection introduces the 2D lidar and 3D lidar sensors mostly targeting indoor environments with poor illumination conditions, with typical robotic application areas to primarily focus on collision avoidance, SLAM, 3D reconstruction, etc.

RPLIDAR A2 is a 360 degree omnidirectional 2D lidar, which provides 16000 samples per second, with the maximum range of 25 m.

RPLIDAR S1 is a 360 degree omnidirectional 2D lidar that provides 9200 samples per second, with a maximum range of 40 m.

Velodyne Puck Lite has been designed for applications that demand a lower weight, while it provides a 100 m range with 360 degree  $\times$  30 degree horizontal and vertical field of view. The full 360-degree environmental view is an ideal capacity to deliver accurate real-time 3D data in multiple robotic applications.

## 2.3. Inertial measurement unit

IMUs are the main core of the localization for robotic applications in a variety of applications, from under-water, to ground, aerial and space robotics. Their orientation, linear and angular accelerations are fundamental for most of the data fusion methods.

VectorNav VN-100 is a small size IMU unit with the weight of 15 g, which provides 3-axis accelerometers, gyros, and magnetometers, and barometric pressure. Furthermore, the VN-100

provides up to 400 Hz rate filtered data, and RMS of  $0.5^\circ$  and  $2.0^\circ$  for heading (magnetic) and pitch/roll measurements. For the installation of the Vecton Nav, damping vibration dampers should be used to reduce the frame vibration affect on the IMU measurements.

## 2.4. UWB ranging sensor

Ultra wideband (UWB) is a short-range radio technology which can be used for distance measurements. In this study UWB system is used to provide additional measurement source (ground truth) for robot position estimation. The positioning is acquired with the help of at least three nodes (trilateration) positioned strategically as anchors to localize the robot in 3D space. The accuracy of the relative position between the anchors directly affects the accuracy of the robot localization. These positions need to be entered in the software provided by the manufacturer to configure the anchors since the technology used to localize the object is based on the time of flight (ToF) method. The hardware UWB nodes used in the dataset were the Decawave MDEK1001, which additionally incorporate a 3-axis accelerometer. The UWB node has size of  $19.1 \text{ mm} \times 26.2 \text{ mm} \times 2.6 \text{ mm}$  and uses a 6.8 Mbps data rate IEEE802.15.4-2011 UWB compliant communication protocol. The Decawave MDEK1001 positioning system has an accuracy of less than 10 cm [20] provided that the accuracy of the placement of the anchors is within a few centimeters.

## 3. Field test description

The dataset was collected from an underground tunnel in Luleå, Sweden. This is a challenging environment for SLAM algorithms in terms of lightning conditions, dust particles and high humidity. Fig. 1 represents the images from tunnel's different locations. Its map, that was generated from the 3D lidar measurements is shown in Fig. 3. The dataset was recorded in three incremental batches for three sensors' sets, while Pioneer velocity was set to 1 m/s. During the experiment, the operator keeps the platform in middle of the tunnel to have approximately same distance between the two walls. Starting the traverse in point A and finishing it in point B, with further continuation through the roundabout to point C and completing the traverse at point D. A detailed description of each location and related sensor measurements are summarized in Table 3.

Obtaining the ground truth in harsh SubT environments is a challenging task. For this purpose, in the tunnel area C, it was deployed an UWB positioning system, which consists of four UWB

**Table 2**  
Specification of all the sensors in the data collection platform.

Sensor	Field of view, [degrees]	Dimensions, WxHxD, [mm]	Weight, [gram]
Vectornav VN-100	–	36 × 33 × 9	15
Rplidar A2	360°, horizontal plane		190
Rplidar S1	360°, horizontal plane	55.5 × 55.5 × 51	105
Velodyne Puck Lite	360° × 30° horizontal × vertical FOV		590
FLIR Boson 640	95° (HFOV) 4.9 mm	21 × 21 × 11 (without lens)	140
Intel RealSense T265	Two Fisheye lenses with combined 163±5° FOV	108 × 24.5 × 12.5	55
Intel RealSense D455	Depth Field of View (FOV): 86° × 57° (±3°) RGB sensor FOV (H × V): 86 × 57° (±3)	124 × 29 × 26	103
Prophece event trigger camera	Diagonal FOV: 70	60 × 50 × 78	140
Decawave MDEK1001	–	19.1 × 26.2 × 2.6	41
Insta 360 EVO	Spherical	50.3 × 49 × 52.54	113
GoPro Hero 7	Horizontal FOV 94.4 Vertical FOV 122.6	62 × 28 × 4.5	92.4

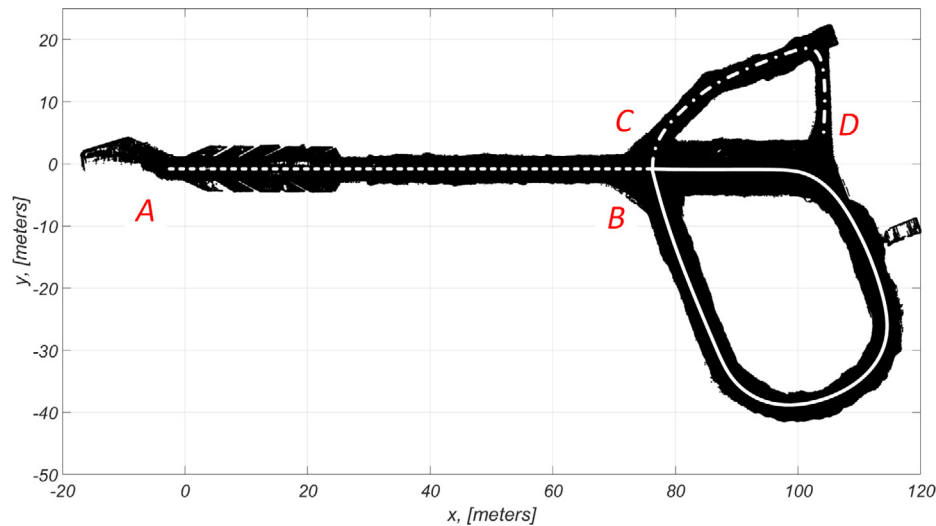


**Fig. 3.** A top view of the map generated from the 3D lidar scans from the field test environment. Dashed line represents the traverse from point A to B, solid line represents the traverse from point B through the roundabout to point C and dash-dotted line shows the traverse from point C to D.

anchors and allows to estimate the robot position in the world frame  $w$ . The UWB setup is depicted in Fig. 4. During the data collection process was used UWB configuration with four anchors and one tag. For obtaining positioning information with up to 10 cm accuracy, the anchors were first placed in the tunnel within the line-of-sight, secondly their positions were measured to cm accuracy and entered in the Decawave software.

#### 4. Data format and synchronization

In this Section the dataset format, notations and calibration parameters are introduced.

##### 4.1. Conventions and notations

In the data collection platform, all sensor are mechanically attached and the whole structure is assumed to have a rigid body. Sensors' reference frames are depicted in Fig. 2(a). In it, the IMU frame is set as a base frame  $b$ . Its  $x$ -axis is aligned with robot

forward direction,  $y$ -axis is pointing right and  $z$ -axis is pointing down. All other sensors are fixed by a mechanical design and their translations  $\mathbf{p} = [x, y, z]$  and rotations  $\mathbf{r} = [\phi, \theta, \psi]$  are defined and aligned with respect to the IMU frame. The  $\phi, \theta, \psi$  are Euler angles and define roll, pitch and yaw respectfully. The precise summary of sensors' frames definitions is shown in Table 4, additionally the sensor suite setup<sup>6</sup> is provided in unified robot description format (URDF).

It should be also noted that all the sensorial measurements are represented in the international system of units, while the timestamps are in the Unix time format.

##### 4.2. Data format

The dataset contains data stored in ROS bag<sup>7</sup> files and video feed formats from three consecutive tunnel locations, and each

<sup>6</sup> [Sensor\\_suite.urdf.xacro](#)

<sup>7</sup> <http://wiki.ros.org/Bags>

**Table 3**

Data description.

Data sequence	Location (Fig. 3)	Notes
<b>Sensor set 1:</b> PUCK LITE AND VN-100		
00S – 112S	A - B	This is a start file of the dataset and data batch. In it, the robot is facing towards B location. The tunnel area is pitch black and contains moisture on walls and ground.
00S – 186S	B - C	The robot is facing towards the distant entrance of the roundabout. The tunnel area is dark and has illumination from 90S.
00S – 128S	C - D	The robot is facing forward towards D location. The tunnel area is pitch black. The data batch ends when robot reaches location.
<b>Sensor set 2:</b> PUCK LITE, A2, S1, REALSENSE T265, BOSON 640, EVENT TRIGGER CAMERA, MDEK1001 AND VN-100		
00S – 109S	A - B	This is a start file of the data batch. In it, the robot is facing towards B location. The tunnel area is pitch black and contains moisture on walls and ground. UWB information is not available.
00S – 181S	B - C	The robot is facing towards the distant entrance of the roundabout. The tunnel area is dark and has illumination from 85S. UWB information is available between 0S and 30S and from 160S
00S – 84S	C - D	The robot is facing forward towards D location. The tunnel area is pitch black. UWB information is available up to 25S. The data batch ends when robot reaches location D.
<b>Sensor set 3:</b> A2, S1, REALSENSE D455 AND T265, BOSON 640, EVENT TRIGGER CAMERA AND VN-100		
00S – 107S	A - B <sup>a</sup>	This is a start file of the dataset and data batch. In it, the robot is facing towards B location. The tunnel area is pitch black and contains moisture on walls and ground.
00S – 180S	B - C <sup>a</sup>	The robot is facing towards the distant entrance of the roundabout. The tunnel area is dark and has illumination from 84S.
00S – 75S	C - D <sup>a</sup>	The robot is facing forward towards D location. The tunnel area is pitch black. The data batch and dataset end when robot reaches location D.

<sup>a</sup>D455 provides data measurements with RGB, infrared and depth cameras, while T265 provides data measurements from a single fisheye camera. Their data descriptions are presented in Section 4.

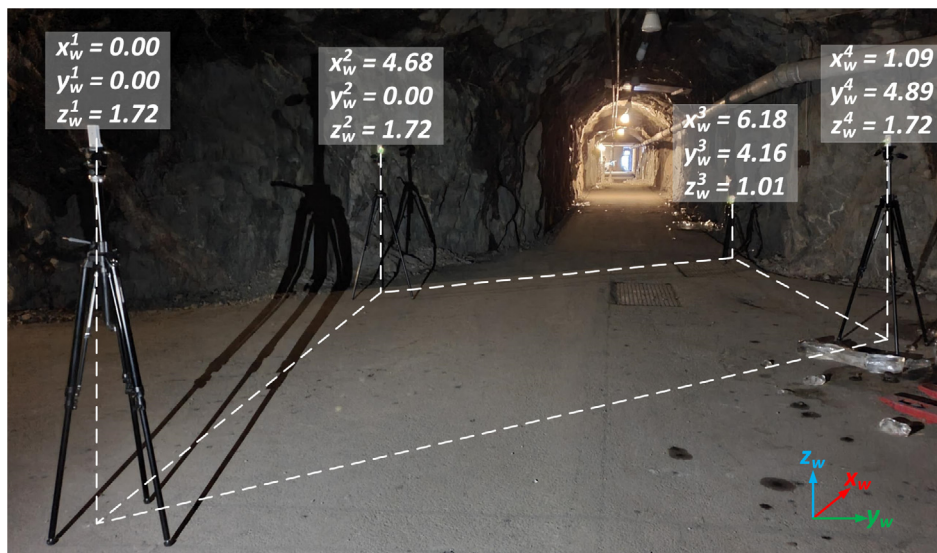


**Fig. 4.** The UWB positioning system deployed in the location C of the underground tunnel. Subscript  $w$  – represents the world frame, while the superscript  $i = [1, 2, 3, 4]$  – represents UWB anchor number.

**Table 4**  
Static transformation frames for each sensor in data collection platform.

Sensor	Frame defined in ROS	Translation, [meters]	Rotations (roll, pitch, yaw) [rad]
Vectornav VN-100 <sup>a</sup>	base_link	$\mathbf{p}_b = [0.00 \ 0.00 \ 0.00]$ ,	$\mathbf{r}_b = [3.14 \ 0.00 \ 0.00]$
Rplidar A2 <sup>b</sup>	laserA2	$\mathbf{p}_1^{b,1} = [0.00 \ 0.00 \ 0.09]$ ,	$\mathbf{r}_{b,1} = [0.00 \ 0.00 \ 3.14]$
Rplidar S1 <sup>b</sup>	laserS1	$\mathbf{p}_2^{b,2} = [0.00 \ 0.00 \ 0.17]$ ,	$\mathbf{r}_{b,2} = [0.00 \ 0.00 \ 3.14]$
Velodyne Puck Lite <sup>c</sup>	velodyne	$\mathbf{p}_3^{b,3} = [0.00 \ 0.00 \ 0.28]$ ,	$\mathbf{r}_{b,3} = [0.00 \ 0.00 \ 0.00]$
FLIR Boson 640 <sup>b</sup>	boson_camera	$\mathbf{p}_4^{b,4} = [0.00 \ -0.16 \ 0.02]$ ,	$\mathbf{r}_{b,4} = [0.00 \ 0.00 \ 0.00]$
Intel RealSense T265 <sup>b</sup>	T265_link	$\mathbf{p}_5^{b,5} = [0.07 \ 0.00 \ 0.22]$ ,	$\mathbf{r}_{b,5} = [0.00 \ 0.00 \ 0.00]$
Intel RealSense D455 <sup>d</sup>	D455_link	$\mathbf{p}_6^{b,6} = [0.08 \ -0.05 \ 0.13]$ ,	$\mathbf{r}_{b,6} = [0.00 \ 0.00 \ 0.00]$
Prophesee event trigger camera <sup>b</sup>	Prophesee Camera_optical_frame	$\mathbf{p}_7^{b,7} = [0.01 \ 0.16 \ 0.01]$ ,	$\mathbf{r}_{b,7} = [0.00 \ 0.00 \ 0.00]$
Decawave MDEK1001 <sup>e</sup>	Decawave	$\mathbf{p}_8^{b,8} = [-0.08 \ 0.00 \ 0.35]$ ,	$\mathbf{r}_{b,8} = [0.00 \ 0.00 \ 3.14]$
Insta 360 EVO	-	$\mathbf{p}_9^{b,9} = [0.00 \ 0.00 \ -0.38]$ ,	$\mathbf{r}_{b,9} = [0.00 \ 0.00 \ 0.00]$
GoPro Hero 7	-	$\mathbf{p}_{10}^{b,10} = [0.09 \ 0.00 \ 0.02]$ ,	$\mathbf{r}_{b,10} = [0.00 \ 0.00 \ 0.00]$

<sup>a</sup>Sensor set 1, 2 and 3.

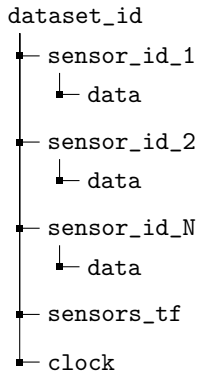
<sup>b</sup>Sensor set 2 and 3.

<sup>c</sup>Sensor set 1 and 2.

<sup>d</sup>Sensor set 3.

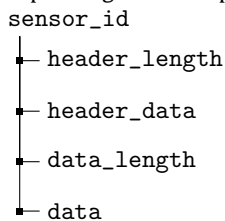
<sup>e</sup>Sensor set 2.

location contains measurements from multiple sensors as it is shown in Table 3. This file format is used for storing, processing, analysing and visualizing ROS message data, such as text, images, positions, orientations, etc, that are published by sensors through ROS topics.<sup>8</sup> Measurements from each sensor are grouped under the related topic<sup>9</sup> and namespace, such that a generic message structure can be represented as



where  $N$  corresponds to the number of sensors, while the time synchronization of all sensors measurements within a bag file is established using timestamps and the `/clock` topic.<sup>10</sup>

Each sensor topic in bag file has a following structure with a corresponding timestamp:



The dataset root folder contains folders named as *Sensor\_set\_id*, where  $id = [1, 2, 3]$  represents the correspondent sensors set.

Each sensor folder contains sub-folders with bag files for each location as defined in Table 3. ROS bag files are named as follows: *sensor\_set\_id\_timestamp*. The video feed files are placed in the dataset root folder named *Videos*, which contains sub-folders for GoPro and 360Evo. The video files are named as with respect to location.

The Vectornav VN-100 sensor measurements are grouped under the *vectornav* namespace and provide IMU measurements in the following topic:

Sensor	Rate	ROS message type
[IMU]	200Hz	[sensor_msgs/Imu]

Rplidar A2 and S1 messages are grouped under the related A2 and S1 namespaces and provide measurements in topic:

Sensor	Rate	ROS message type
[A2/scan]	10Hz	[sensor_msgs/LaserScan]
[S1/scan]	10Hz	[sensor_msgs/LaserScan]

Velodyne Puck Lite provides 3D scan data in a point cloud format and 2D scan data in a laser scan format in the following topics:

Sensor	Rate	ROS message type
[velodyne_points]	10Hz	[sensor_msgs/PointCloud2]
[scan]	10Hz	[sensor_msgs/LaserScan]

FLIR Boson 640 messages are grouped under the *flir\_boson* namespace and provide thermal measurements in topic:

Sensor	Rate	ROS message type
[flir_boson/image_raw]	30Hz	[sensor_msgs/Image]

Intel RealSenses sensor messages from T265 and D455 are grouped under the *T265* and *D455* namespaces and provide measurements in the following topics

<sup>8</sup> <http://wiki.ros.org/rostopic>

<sup>9</sup> <http://wiki.ros.org/Topics>

<sup>10</sup> <http://wiki.ros.org/Clock>

```
[T265]
Sensor      Rate  ROS message type
[accel/
  sample]   63Hz  [sensor_msgs/Imu]
[gyro/
  sample]   200Hz [sensor_msgs/Imu]
[fisheye1/
  image_raw] 30Hz  [sensor_msgs/Image]
[fisheye2/
  image_raw] 30Hz  [sensor_msgs/Image]
```

```
[D455]
Sensor      Rate  ROS message type
[color/
  image_raw] 7Hz  [sensor_msgs/Image]
[depth/
  image_rect_raw] 52Hz  [sensor_msgs/Image]
[infra1/
  image_rect_raw] 30Hz  [sensor_msgs/Image]
[aligned_depth_to_color/
  image_raw] 7Hz  [sensor_msgs/Image]
```

Prophesee messages are grouped under the *prophesee* namespace and provide measurements in topic

```
Sensor      Rate  ROS message type
[camera/
  cd_events_buffer] 1600Hz  EventArray
```

To access the event camera data the correspondent ROS package<sup>11</sup> has to be installed.

UWB messages are grouped under the *dwm1001* namespace and provide measurements from UWB tag and anchors in the following topics

```
[tag]
Sensor      Rate  ROS message type
[tag/position] 10Hz  [geometry_msgs/
  PoseStamped]

[tag/to/anchor/AN0/
  distance] 10Hz  [std_msgs/Float64]
[tag/to/anchor/AN1/
  distance] 10Hz  [std_msgs/Float64]
[tag/to/anchor/AN2/
  distance] 10Hz  [std_msgs/Float64]
[tag/to/anchor/AN3/
  distance] 10Hz  [std_msgs/Float64]
```

For previewing the tunnel environment, RGB video feeds from Gopro Hero7 and Insta 360Evo cameras are provided with the following specifications

Sensor	Resolution	Rate	Format
[Hero7]	[1920 x 1440]	29.97 FPS	[MPEG-4]
[360Evo]	[5760 x 2880]	29.97 FPS	[MPEG-4]

#### 4.3. Data usage

The dataset can be downloaded from [Dataset](#). It was recorded in Ubuntu 18.04 LTS with ROS Melodic. To access and analyse sensor data in the bag files, ROS has a built-in set of tools called *roslaunch*,<sup>12</sup> which provides a set of commands for easy data access. Additionally, for the cases when it is required to have processing

time synchronized with sensor data timestamps, as they were recorded, a clock server topic `/clock` should be used. In order to enable time synchronization it is required to set the parameter `/use_sim_time = true` and to play a bag file using the `--clock` option. The data can be accessed both from individual bag files as `roslaunch sensor_set_id_timestamp.bag` and from multiple bag files as `roslaunch sensor_set_id_timestamp*`.

#### Declaration of competing interest

The authors declare that they have no known competing financial interests or personal relationships that could have appeared to influence the work reported in this paper.

#### References

- [1] A. Agha, K. Otsu, B. Morrell, D.D. Fan, R. Thakker, A. Santamaria-Navarro, S. Kim, A. Bouman, X. Lei, J.A. Edlund, M.F. Ginting, K. Ebadi, M. Anderson, T. Pailevanian, E. Terry, M.T. Wolf, A. Tagliabue, T.S. Vaquero, M. Palieri, S. Tepsuporn, Y. Chang, A. Kalantari, F. Chavez, B.T. Lopez, N. Funabiki, G. Miles, T. Touma, A. Buscicchio, J. Tordesillas, N. Alatur, J. Nash, W. Walsh, S. Jung, H. Lee, C. Kanellakis, J. Mayo, S. Harper, M. Kaufmann, A. Dixit, G. Correa, C. Lee, J. Gao, G. Merewether, J. Maldonado-Contreras, G. Salhotra, M.S. da Silva, B. Ramtoula, Y. Kubo, S.A. Fakoorian, A. Hatteland, T. Kim, T. Bartlett, A. Stephens, L. Kim, C. Bergh, E. Heiden, T. Lew, A. Cauligi, T. Heywood, A. Kramer, H.A. Leopold, H.C. Choi, S. Daftry, O. Toupet, I. Wee, A. Thakur, M. Feras, G. Beltrame, G. Nikolakopoulos, D.H. Shim, L. Carlone, J. Burdick, NeBula: Quest for robotic autonomy in challenging environments; TEAM CoSTAR at the DARPA subterranean challenge, 2021, pp. 1–77, <http://dx.doi.org/10.48550/arXiv.2103.11470>, CoRR abs/2103.11470, arXiv:2103.11470.
- [2] S.S. Mansouri, C. Kanellakis, E. Fresk, B. Lindqvist, D. Kominiak, A. Koval, P. Sopasakis, G. Nikolakopoulos, Subterranean MAV navigation based on nonlinear MPC with collision avoidance constraints, IFAC-PapersOnLine 53 (2) (2020) 9650–9657, <http://dx.doi.org/10.1016/j.ifacol.2020.12.2612>.
- [3] S.S. Mansouri, C. Kanellakis, D. Kominiak, G. Nikolakopoulos, Deploying MAVs for autonomous navigation in dark underground mine environments, Robot. Auton. Syst. (2020) 1–15, <http://dx.doi.org/10.1016/j.robot.2020.103472>.
- [4] DARPA, DARPA Subterranean (SubT) challenge, 2021, URL <https://www.subtchallenge.com/>. (Accessed March 2022).
- [5] DARPA, DARPA Subterranean (SubT) challenge, 2020, URL <https://www.darpa.mil/program/darpa-subterranean-challenge>. (Accessed March 2022).
- [6] M. Tranzatto, F. Mascari, L. Bernreiter, C. Godinho, M. Camurri, S. Khattak, T. Dang, V. Reijgwart, J. Loeje, D. Wisth, S. Zimmermann, H. Nguyen, M. Fehr, L. Solanka, R. Buchanan, M. Bjelonic, N. Khedekar, M. Valceschini, F. Jenelten, M. Dharmadhikari, T. Homberger, P.D. Petris, L. Wellhausen, M. Kulkarni, T. Miki, S. Hirsch, M. Montenegro, C. Papachristos, F. Tresoldi, J. Carius, G. Valsecchi, J. Lee, K. Meyer, X. Wu, J.I. Nieto, A. Smith, M. Hutter, R. Siegwart, M.W. Mueller, M.F. Fallon, K. Alexis, CERBERUS: autonomous legged and aerial robotic exploration in the tunnel and urban circuits of the DARPA subterranean challenge, 2022, pp. 1–50, <http://dx.doi.org/10.48550/arXiv.2201.07067>, CoRR abs/2201.07067, arXiv:2201.07067.
- [7] N. Hudson, F. Talbot, M. Cox, J.L. Williams, T. Hines, A. Pitt, B. Wood, D. Frousheger, K.L. Surdo, T. Molnar, R. Steindl, M. Wildie, I. Sa, N. Kottege, K. Stephanas, E. Hernández, G. Catt, W. Docherty, B. Tidd, B. Tam, S. Murrell, M. Bessell, L. Hanson, L. Tychsen-Smith, H. Suzuki, L. Overs, F. Kendoul, G. Wagner, D. Palmer, P. Milani, M. O'Brien, S. Jiang, S. Chen, R.C. Arkin, Heterogeneous ground and air platforms, homogeneous sensing: Team CSIRO data61's approach to the DARPA subterranean challenge, 2021, pp. 1–50, <http://dx.doi.org/10.48550/arXiv.2104.09053>, CoRR abs/2104.09053, arXiv:2104.09053.
- [8] M.T. Ohradzansky, E.R. Rush, D.G. Riley, A.B. Mills, S. Ahmad, S. McGuire, H. Biggie, K. Harlow, M.J. Miles, E.W. Frew, C. Heckman, J.S. Humbert, Multi-agent autonomy: Advancements and challenges in subterranean exploration, 2021, pp. 1–39, <http://dx.doi.org/10.48550/arXiv.2110.04390>, CoRR abs/2110.04390, arXiv:2110.04390.
- [9] B. Li, C. Wang, P. Reddy, S. Kim, S. Scherer, Airdet: Few-shot detection without fine-tuning for autonomous exploration, 2021, pp. 1–23, <http://dx.doi.org/10.48550/arXiv.2112.01740>, CoRR abs/2112.01740, arXiv:2112.01740.
- [10] T. Roucek, M. Pecka, P. Cizek, T. Petricek, J. Bayer, V. Salansky, T. Azayev, D. Hert, M. Petrlik, T. Baca, V. Spurny, V. Kratký, P. Petracek, D. Baril, M. Vaidis, V. Kubelka, F. Pomerleau, J. Faigl, K. Zimmermann, M. Saska, T. Svoboda,

<sup>11</sup> [https://github.com/prophesee-ai/prophesee\\_ros\\_wrapper](https://github.com/prophesee-ai/prophesee_ros_wrapper)

<sup>12</sup> <http://wiki.ros.org/roslaunch>

- T. Krajník, System for multi-robotic exploration of underground environments CTU-CRAS-NORLAB in the DARPA subterranean challenge, 2021, pp. 1–50, <http://dx.doi.org/10.48550/arXiv.2110.05911>, CoRR abs/2110.05911, arXiv:2110.05911.
- [11] IEEE Spectrum, DARPA Subt finals: Meet the teams, 2021, URL <https://spectrum.ieee.org/darpa-subterranean-challenge/>. (Accessed March 2022).
- [12] K. Leung, D. Lühr, H. Houshiar, F. Inostroza, D. Borrmann, M. Adams, A. Nüchter, J. Ruiz del Solar, Chilean underground mine dataset, Int. J. Robot. Res. 36 (1) (2017) 16–23, <http://dx.doi.org/10.1177/0278364916679497>.
- [13] M. Magnusson, A. Nüchter, C. Lörken, 3D robotic scan repository, kvarntorp mine, 2015, URL <http://kos.informatik.uni-osnabrueck.de/3Dscans/>. (Accessed March 2022).
- [14] M. Kasper, S. McGuire, C. Heckman, A benchmark for visual-inertial odometry systems employing onboard illumination, in: 2019 IEEE/RSJ International Conference on Intelligent Robots and Systems, IROS, IEEE, 2019, pp. 5256–5263, <http://dx.doi.org/10.1109/IROS40897.2019.8968554>.
- [15] CTU-CRAS-NORLAB team, Tunnel-circuit subterranean (SubT) challenge, 2019, URL <http://robotics.fel.cvut.cz/cras/darpa-subt/>. (Accessed March 2022).
- [16] C. Wang, W. Wang, Y. Qiu, Y. Hu, S. Scherer, Visual memorability for robotic interestingness via unsupervised online learning, in: European Conference on Computer Vision, ECCV, Springer, 2020, pp. 52–68, [http://dx.doi.org/10.1007/978-3-030-58536-5\\_4](http://dx.doi.org/10.1007/978-3-030-58536-5_4).
- [17] J.G. Rogers, J.M. Gregory, J. Fink, E. Stump, Test your SLAM! the subt-tunnel dataset and metric for mapping, in: 2020 IEEE International Conference on Robotics and Automation, ICRA, IEEE, 2020, pp. 955–961, <http://dx.doi.org/10.1109/ICRA40945.2020.9197156>.
- [18] J.G. Rogers, A. Schang, C. Nieto-Granda, J. Ware, J. Carter, J. Fink, E. Stump, The DARPA subt urban circuit mapping dataset and evaluation metric, in: International Symposium on Experimental Robotics, Vol.19, Springer, 2021, pp. 391–401, [http://dx.doi.org/10.1007/978-3-030-71151-1\\_35](http://dx.doi.org/10.1007/978-3-030-71151-1_35).
- [19] Team CERBERUS, ARL: Subt-Edu, 2019, URL <https://www.autonomousrobotslab.com/subt-edu.html>. (Accessed March 2022).
- [20] Decawave, MDEK1001 Product brief, 2017, URL <https://www.decawave.com/mdek1001/productbrief/>. (Accessed March 2022).



**Anton Koval** is a post-doctoral researcher at the Department of Computer Science, Electrical and Space Engineering at the Luleå University of Technology, Sweden. He received his Ph.D. from National Technical University of Ukraine “Kyiv Polytechnic Institute”, Ukraine in 2012. He has been involved in several European and Ukrainian National projects on micro aerial vehicles and environmental monitoring. In 2018 he received the Swedish Institute Visby scholarship for senior scientists for 6 months at Luleå University of Technology, Sweden. His current research interests are mainly focused on control, exploration and path planning with multiple agents.



**Samuel Karlsson** received a Master in Computer Science and Engineering at Luleå University of Technology (LTU), Luleå, Sweden, in 2020. He is currently a Ph.D. student in the Control Engineering Group, Department of Computer Science, Electrical Engineering and Space Engineering, LTU. He works in the field of robotics, focusing on path planning and mapping with multiple agents.



**Sina Sharif Mansouri** (Member, IEEE) received the Bachelor of Science degree from the University of Tehran, Iran, in 2012, the Master of Science degree from the Technical University of Dortmund, Germany, in 2014, and the Ph.D. degree from the Control Engineering Group, Luleå University of Technology (LTU), Luleå, Sweden, in 2020. He is currently a Postdoctoral Researcher within the Control Engineering Group, Department of Computer Science, Electrical and Space Engineering, LTU. He also works in the field of robotics, focusing on control, navigation, and exploration with

multiple agents.



**Christoforos Kanellakis** received the Ph.D. degree from the Control Engineering Group, Luleå University of Technology (LTU), Sweden, and the Diploma degree from the Department of Electrical and Computer Engineering, University of Patras (UPAT), Greece, in 2015. He is currently a Postdoctoral Researcher with the Department of Computer Science, Electrical and Space Engineering, LTU. He also works in the field of robotics, focusing on the combination of control and vision to enable robots perceive and interact with the environment.



**Ilias Tevetzidis** received the Bachelor's degree in Automotive Engineering from the Luleå University of Technology, Sweden, in 2020. He is currently a Technician within the Robotics and Artificial Intelligence Group, Department of Computer Science, Electrical and Space Engineering, LTU. His main interest is robotics and mechatronics.



**Jakub Haluška** received the Bachelor's degree in Mechanical Engineering from the Technical University of Liberec, Czech Republic, in 2016. The Bachelor's degree in Mechanical Engineering degree from the Technical University of Liberec, Czech Republic, in 2019. He is currently a Research Engineer within the Control Engineering Group, Department of Computer Science, Electrical and Space Engineering, LTU. His main interest is the design and construction of robots.



**Ali-akbar Agha-mohammadi** is a robotics research technologist with NASA's Jet Propulsion Laboratory (JPL), Caltech. Previously, he was an autonomy research engineer with Qualcomm Research and a postdoctoral researcher with the Laboratory for Information and Decision Systems at Massachusetts Institute of Technology. He received his Ph.D. from Texas A&M University, and his research interests include robotic autonomy, mobility and perception, stochastic control systems and filtering theory. Agha manages several projects at JPL on autonomy, control and perception for robotic systems (rovers and aerial vehicles). He was selected as a NASA NIAC Fellow in 2018.



**George Nikolakopoulos** was working as a Project Manager and a Principal Investigator in several R&D&I projects funded by the EU, ESA, Swedish, and the Greek National Ministry of Research. In 2013, he has established the bigger outdoors motion capture systems in Sweden, and most probably in Europe, as part of the FROST Field Robotics Laboratory, Luleå University of Technology, Luleå, Sweden. He is currently a Professor on robotics and automation with the Department of Computer Science, Electrical and Space Engineering, Luleå University of Technology. His work is focusing in the area of robotics and control applications, while he has a significantly large experience in creating and managing European and National Research Projects. He is the Coordinator of H2020-ICT AEROWORKS project in the field of aerial collaborative UAVs and H2020-SPIRE project DISIRE in the field of integrated process control. His published scientific work includes more than 150 published international journals and conferences in the fields of his interest. In 2003, he has received the Information Societies Technologies (IST) Prize Award for the Best Paper that promotes the scopes of the European IST (currently known as ICT) sector. In 2014, he has received the 2014 Premium Award for Best Paper in IET Control Theory and Applications, (Elsevier) for the research work in the area of UAVs. In 2014, he has been nominated as a LTU's Wallenberg candidate, one out of three nominations from the University and 16 in total engineering nominations in Sweden. His publications in the field of UAVs have received top recognition from the related scientific community, while have been several times listed in the TOP 25 most popular publications in Control Engineering Practice (Elsevier).